

THE TURBULENT BOUNDARY LAYER IN THE INITIAL SEGMENT  
OF AXISYMMETRIC CHANNELS WHEN FLOW SWIRLING OCCURS  
AT THE INLET

G. V. Filippov and V. G. Shakhov

UDC 532.517.4

We present an approximate solution for the problem of a turbulent boundary layer in an incompressible liquid in the case of flow swirling at the inlet.

The twisted flow of a liquid in channels is used in a variety of equipment and installations.

The frictional losses are one of the fundamental factors governing the energy expended on the movement of the working fluid through the channels. The development of a boundary layer at the walls of the channel leads to a change in the pressure recovery factor which is an indication of channel efficiency. Equally important is the determination of the point of separation.

To determine the above-enumerated characteristics, we should examine the flow of a viscous liquid.

In actual practice we usually deal with flows having a turbulent boundary layer at a solid surface. A theoretical investigation of such flows is found in [1-3].

However, in the cited literature we find indications only of the possibility of a basic solution for such problems and no quantitative estimates are given for the effect of flow swirling. Moreover, the authors assume an approximate flow model in a nonviscous core, assuming it should be potential, with the vortex situated along the channel axis, which is a special form of swirling.

Below we present an approximate solution for the problem of the turbulent boundary layer in an incompressible liquid for the case of flow swirling at the channel inlet. Consideration has been given to the effect of the transverse curvature of the solid surface on the boundary layer and to the mutual effect of the transverse and longitudinal components of the coefficients of turbulent friction and the velocity profiles in the boundary layer. A number of quantitative estimates are given. No limitation has been imposed on the form of the swirling.

1. Integral Relationships for the Boundary Layer. The equations of motion in the boundary layer in a cylindrical coordinate system, with consideration of axial symmetry, has the following form [4]:

$$\begin{aligned} u \frac{\partial u}{\partial x} + v \frac{\partial u}{\partial r} &= -\frac{1}{\rho} \frac{\partial p}{\partial x} + \frac{1}{\rho r} \frac{\partial (r\tau_1)}{\partial r}, \\ u \frac{\partial w}{\partial x} + v \frac{\partial w}{\partial r} + \frac{vw}{r} &= \frac{1}{\rho r^2} \frac{\partial (r^2\tau_2)}{\partial r}, \\ \frac{\partial p}{\partial r} &= \rho \frac{w^2}{r}, \quad \frac{\partial (ru)}{\partial x} + \frac{\partial (rv)}{\partial r} = 0. \end{aligned} \tag{1}$$

The boundary conditions

$$\begin{aligned} r = R, \quad u = v = w = 0, \\ r = R - \delta, \quad u = U, \quad w = w_0. \end{aligned} \tag{2}$$

Neglecting the effect of rotation on the transverse pressure gradient in the boundary layer (since in the initial segment where the swirling is intensive the thickness of the layer is small, and where the thickness

---

Korolev Aviation Institute, Kuibyshev. Translated from *Inzhenerno-Fizicheskii Zhurnal*, Vol. 17, No. 1, pp. 95-102, July, 1969. Original article submitted August 7, 1968.

© 1972 Consultants Bureau, a division of Plenum Publishing Corporation, 227 West 17th Street, New York, N. Y. 10011. All rights reserved. This article cannot be reproduced for any purpose whatsoever without permission of the publisher. A copy of this article is available from the publisher for \$15.00.

of the layer is comparable to the tube radius the swirling is weak) and taking into consideration the experimental fact [5, 6]

$$\frac{r^2 v \omega}{r^2 \omega^2} = \frac{v}{\omega} \leq 0.03,$$

we turn in the normal fashion from system (1) to the integral relationship of the boundary layer:

$$\begin{aligned} \frac{d\vartheta_x^{**}}{dx} + \vartheta_x^{**} (2+H) \frac{1}{U} \frac{dU}{dx} &= \frac{R\tau_{10}}{\rho U^2}, \\ \frac{d}{dx} (U\omega_0 R\vartheta_{xy}^{**}) &= -\frac{R^2\tau_{20}}{\rho}, \\ \vartheta_x^{**} &= \int_0^\delta \left(1 - \frac{u}{U}\right) (R-y) dy, \\ \vartheta_{xy}^{**} &= \int_0^\delta \frac{u}{U} \frac{r\omega}{R\omega_0} (R-y) dy, \\ \vartheta_x^{**} &= \int_0^\delta \left(1 - \frac{u}{U}\right) \frac{u}{U} (R-y) dy. \end{aligned} \quad (3)$$

**2. Frictional Stress and Velocity Profiles.** The system of two differential equations (3) contains 5 unknowns ( $\vartheta_x^{**}$ ,  $H$ ,  $\tau_{10}$ ,  $\vartheta_{xy}^{**}$ ,  $\tau_{20}$ ). To close this system we have to establish 3 additional relationships.

We will adopt the Prandtl two-layer boundary-layer model. At some distance from the channel walls we have

$$\tau_1 = -\rho \langle u'v' \rangle, \quad \tau_2 = -\rho \langle w'v' \rangle. \quad (4)$$

On the basis of the results [7] we will assume the following relationships between the frictional stresses and the averaged components of velocity in the boundary layer:

$$\begin{aligned} \tau_1 &= \rho l^2 \sqrt{1 + \left(\frac{\tau_2}{\tau_1}\right)^2} \left(\frac{\partial u}{\partial r}\right)^2, \\ \tau_2 &= \rho l^2 \sqrt{1 + \left(\frac{\tau_1}{\tau_2}\right)^2} \left(\frac{1}{r} \frac{\partial \Gamma}{\partial r}\right)^2. \end{aligned} \quad (5)$$

Since the angle is small, in first approximation we will neglect the effect of the pressure gradient on the velocity profiles. From the condition of equilibrium for the liquid volumes in the boundary layer we will then have

$$r\tau_1 = R\tau_{10}, \quad r^2\tau_2 = R^2\tau_{20}. \quad (6)$$

Assuming  $l = ky$  and integrating (5) with consideration of (6), we have

$$\begin{aligned} u &= \frac{v_{1*}}{k} \int_0^y \frac{\sqrt{R/r}}{\sqrt[4]{1 + A^{-1}(R/r)^2}} \frac{dy}{y} + M_1; \\ \Gamma &= \frac{Rv_{2*}}{k} \int_0^y \frac{1}{\sqrt[4]{1 + A(r/R)^2}} \frac{dy}{y} + M_2. \end{aligned} \quad (7)$$

Since (6) is valid near the wall, i.e., when  $r/R \approx 1$ , in (7) we will assume in binomials that  $r/R = 1$ . Then with consideration of (2) the velocity profiles will be described by the equations

$$\begin{aligned} u^0 &= 1 + \frac{B}{z_1} \ln \frac{(\sqrt{R} - \sqrt{R-y})(\sqrt{R} + \sqrt{R-\delta})}{(1 - \sqrt{R-y})(1 - \sqrt{R-\delta})}; \\ \Gamma^0 &= 1 + \frac{C}{z_2} \ln y^0. \end{aligned} \quad (8)$$

We note that when  $0 \leq A \leq \infty$ :

$$0 \leq B \leq 1, \quad 1 \geq C \geq 0.$$

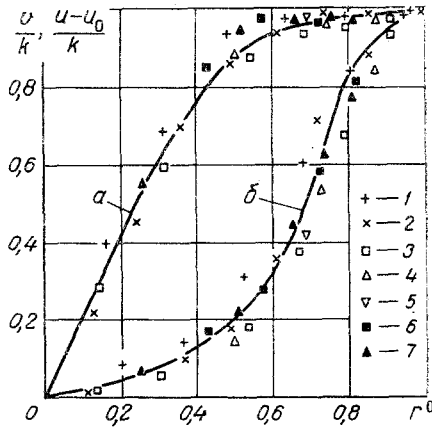


Fig. 1. Distribution of swirling velocity (a) and of the axial velocity (b) outside of the boundary layer on the basis of experimental results [5]: 1)  $Re = 5000$ ; 2)  $10,000$ ; 3)  $15,000$ ; 4)  $20,000$ ; 5)  $25,000$ ,  $(1-5) x^0 = 12$ ; 6)  $25,000$ ,  $x^0 = 24$ ; 7)  $25,000$ ,  $x^0 = 48$ .

equations that  $y = \delta_l = \alpha R / \eta_w$  and equating one with the other, we obtain the relationship between the frictional stress at the surface and the thickness of the boundary layer – the so-called resistance laws:

$$\frac{z_1}{B} = \ln \frac{(1 - \sqrt{1 - \delta/R})(1 + \sqrt{1 - \alpha/\eta_w})}{(1 - \sqrt{1 - \alpha/\eta_w})(1 + \sqrt{1 - \delta/R})} - k\eta_w B \ln \left(1 - \frac{\alpha}{\eta_w}\right),$$

$$\frac{z_2}{C} = \frac{kC\eta_w}{2} \left[1 - \left(1 - \frac{\alpha}{\eta_w}\right)^2\right] - \ln \frac{\alpha}{\eta_w}.$$

When  $B = 1$  the first equations in (9) and (10) coincide with the corresponding equations derived in [8].

As in [8], we will assume that  $k$  and  $\alpha$  are equal to their values for the plane case ( $k = 0.4$ ;  $\alpha = 11.5$ ).

**Conditional Areas.** Since the profiles (8) of the velocity and circulation have been determined, it is not difficult to calculate the conditional areas:

$$\frac{\Phi_x^*}{R_0^2} = \frac{B}{z_1} R^{02} \left( \frac{4}{3} - \sqrt{r^0} - \frac{\sqrt{r^{03}}}{3} \right),$$

$$\frac{\Phi_x^{**}}{R_0^2} = \frac{\Phi_x^*}{R_0^2} + \frac{B^2}{z_1^2} R^{02} \left( \frac{8}{3} \ln f_1 + \frac{8}{3} \ln \frac{\delta}{4R} + \frac{3}{2} \frac{\delta}{R} \right),$$

$$\frac{\Phi_{xy}^{**}}{R_0^2} = -\frac{\Phi_x^*}{R_0^2} + R^{02} \left[ f_2 + \frac{C}{z_2} \left( 1 + \frac{B}{z_1} f_1 \right) f_3 + \frac{BC}{z_1 z_2} f_4 \right],$$

$$f_1 = (1 + \sqrt{r^0}) / (1 - \sqrt{r^0}), \quad f_2 = (1 - r^{02}) / 2,$$

$$f_3 = \frac{\delta}{R} \ln \frac{\delta}{R} \left( 1 - \frac{1}{2} \frac{\delta}{R} \right) - \frac{\delta}{R} \left( 1 - \frac{1}{4} \frac{\delta}{R} \right) + \frac{3}{4},$$

$$f_4 = \ln \frac{\delta}{R} \left( \frac{1}{2} r^{03/2} + r^{01/2} \right) - f_1 \ln \frac{\delta}{R} \ln f_2 - \frac{7\sqrt{r^{03}}}{8}$$

$$- \left[ \left( \frac{1}{4} r^{02} - 1 \right) - \frac{1}{2} \frac{\delta}{R} - \frac{4}{3} \right] \ln f_2 - \frac{25}{12} \sqrt{r^0} - \frac{4}{3} \ln 2 + \frac{71}{24}.$$

When  $B = 1$  the first two equations in (11) are analogous to the corresponding equations in [8].

**5. Reduction of Integral Boundary-Layer Relationships into a System of Integral Equations.** Having presented the functions  $E$  and  $D$  in the form

$$E = E_0 + \Delta E, \quad D = D_0 + \Delta D$$

When  $B = 1$  (the flow is not twisted) the first equation in (8) coincides with the equation for the velocity profile in axisymmetric channels without swirling [8]. When  $C = 1$  (the rotation of the body in a nonmoving medium) the second equation in (8) changes into the profile of the circulation observed experimentally in linear vortices [9].

**3. Resistance Laws.** Equations (8) at the wall (when  $y = 0$ ) do not satisfy the adhesion conditions (2). In accordance with the two-layer boundary-layer model, let us turn to the laminar sublayer. Assuming that the parameters of the latter are functions not only of the technical properties of the liquid and the magnitudes of the frictional stresses at the wall, but also of the transverse curvature of the channel [8], we write the distribution of the velocities in the laminar sublayer in the following form:

$$\frac{u}{v_{1*}} = -B^2 \eta_w \ln \frac{R-y}{R}, \quad \frac{\Gamma}{\Gamma_*} = \frac{C^2 \eta_w}{2} \left[ 1 - \left( 1 - \frac{y}{R} \right)^2 \right],$$

$$\eta_w = \frac{\sqrt{v_{1*}^2 + v_{2*}^2} R}{v} = \frac{k}{B^2} \frac{Re_e}{z_1} = \frac{k}{C^2} \frac{Re_e \alpha}{z_2}.$$

Equations (8) and (9) should be regarded as identically valid at the boundary of the laminar sublayer ( $y = \delta_l$ ). Assuming in these

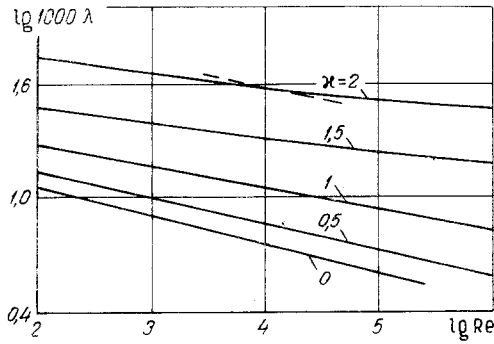


Fig. 2

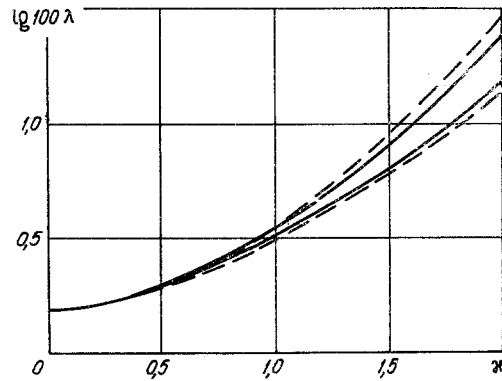


Fig. 3

Fig. 2. Resistance factor for a cylindrical tube. The dashed line shows experimental results [5].

Fig. 3. Resistance factor for a conic diffuser. The dashed lines denote the region of experimental data [6] ( $Re = (1-7) \cdot 10^5$ ); the solid lines represent the theoretical curves, with the upper line representing  $Re = 7 \cdot 10^5$ , and the lower line denoting  $Re = 10^5$ .

and having multiplied the first equation in (3) by  $R^{0D_0} U^{0E_0}$ , after integration we obtain

$$\chi = \frac{1}{U^{0E_0} R^{0D_0}} \left[ D_0 Re \int_{x_0^0}^{x_0^*} (1 + F) U^{0E_0+1} R^{0D_0} dx^0 + \chi_t U_t^{0E_0} R_t^{0D_0} \right], \quad (12)$$

$$F(\chi, P_1, P_2) = D_0^{-1} [P_1 \chi \Delta E + (1 + P_2 \chi) \Delta D].$$

The second equation in (3) is immediately integrated with the aid of the presentation of the function  $L$  in the form  $L = L_0 + \Delta L$ :

$$R_{xy}^{**} = \frac{1}{\chi U^0 R^{0E^2}} \left[ L_0 Re \int_{x_0^0}^{x_0^*} \left( 1 + \frac{\Delta L}{L_0} \right) \chi^2 U^{0E^2} R^{0D_0} dx^0 + R_{xy}^* \chi_t U_t^0 R_t^{0E^2} \right]. \quad (13)$$

Thus we have derived the system of integral equations (12) and (13) to describe the flow in a turbulent boundary layer in the presence of twisting.

For the solution of system (12)-(13) we have to establish the relationships

$$\Delta D = \Delta D(\chi, Re_e, B), \quad \Delta E = \Delta E(\chi, Re_e, B) \text{ and } \Delta L = \Delta L\left(R_{xy}^{**}, B, Re_e, \frac{z_1}{z_2}\right).$$

Functions  $\Delta D$  and  $\Delta E$  are determined from (11) by eliminating  $z_1$ . The function  $\Delta L$  is obtained from (11) through the introduction of the substitution

$$z_1 = \frac{z_2}{\chi} \frac{1}{\sqrt[4]{A}} = \frac{z_2}{\chi} \sqrt[4]{\frac{1-B^4}{B^4}}.$$

**6. A Method of Calculating Flow in a Nonviscous Core.** As was noted earlier, in [1-3] etc., the flow in a nonviscous core is assumed to be potential with the vortex situated at the channel axis. This scheme does not correspond to reality and, moreover, fails to reflect the diversity of twisted flows. It follows from an examination of the experimental results of [5, 6] etc., that the velocity profiles outside of the boundary layer are similar. If we plot  $r_1^0$  along the horizontal axis on the graph, and if we plot  $v_1^0$  or  $u_1^0$  along the vertical axis for the various Reynolds numbers and for the various distances from the inlet, all of the measured points will line up near the general curves (Fig. 1). Consequently, the swirling velocity for a nonviscous flow core and the longitudinal surface within the flow core in the first approximation can be chosen in the form

$$v = k_1(x) f(r), \quad u = u_0(x) + k_1(x) \varphi(r).$$

The functions  $f(r)$  and  $\varphi(r)$  are determined by the design of the diffuser assembly and may be assumed to be known. The functions  $k_1(x)$  and  $u_0(x)$  are found from the condition of a constant flow rate and the conservation of angular momentum, with consideration given to the effect of the frictional forces in the boundary layer.

7. The Simplified Method. We see from (12) that it is associated with (13) only in terms of the parameter  $B$ .

If we denote

$$z_1^0 = z_1/B,$$

the first two equations in (11) will be analogous to the corresponding equations for flow in a channel without twisting [8], and the first equation (10) assumes the form

$$z_1^0 = \ln \frac{(1 - \sqrt{1 - \delta/R})(1 + \sqrt{1 - \alpha/\eta_w})}{(1 - \sqrt{1 - \alpha/\eta_w})(1 + \sqrt{1 - \delta/R})} - k\eta_w B \ln \left( 1 - \frac{\alpha}{\eta_w} \right). \quad (14)$$

The latter is distinguished from the corresponding equation in [8] by the factor  $B$  in the second term of the right-hand member.

For a low twisting ratio ( $\kappa < 2.0$ )  $B$  is a little different from unity. Therefore, if we assume in (14) that  $B = 1$ , it will be identical to the corresponding equation for the case of untwisted flow in which  $z_1$  has been replaced by  $z_1^0$ . Consequently

$$\chi/\chi_0 = 1. \quad (15)$$

Recalling the definition of  $\chi$ , from (15) we obtain

$$c_f = \frac{c_{f0}}{B^2} \frac{R_x^{**}}{R_{x0}^{**}}. \quad (16)$$

It has turned out to be possible, on the basis of a series of calculations, to approximate  $R_x^{**}$  and  $R_{x0}^{**}$  by means of the equations

$$\lg R_x^{**} = \lg M_3 + nz_1^0 + M_4 \lg \text{Re}, \quad (17)$$

$$\lg R_{x0}^{**} = \lg M_3 + nz_1 + M_4 \lg \text{Re}.$$

For the case in which a flat plate is streamlined when  $\text{Re} > 10^2$  we can assume in approximate terms that

$$z_1 = 0.21 + 1.74 \lg \text{Re}. \quad (18)$$

Since according to [7]  $A \approx \kappa^{-2}$ , we have  $B \approx (1 + \kappa^2)^{-1/4}$ . With consideration of (17) and (18) it then follows from (16) that

$$c_f = \Lambda c_{f0}, \quad (19)$$

$$\Lambda(\text{Re}, \kappa) = \frac{1}{1 + \kappa^2} \exp [0.442(0.26 + 1.74 \lg \text{Re}) (\sqrt[4]{1 + \kappa^2} - 1)].$$

8. Comparison with Experiment. The experimental data on the detailed investigation of the type of flow under consideration are extremely limited. For comparison with calculations based on the proposed method we use [5] and [6], which gives the resistance factor as a function of  $\kappa$  and  $\text{Re}$ , as well as the velocity profiles.

Figure 2 shows the change in the resistance factor  $\lambda$  in the case of a twisted liquid flow in a cylindrical tube. On comparison with experiment [5], the initial value of  $\kappa_0$  was determined by extrapolation from the point  $x^0 = 12, 24, 48,$  and  $84$  to the point  $x^0 = 0$ . We took the average value of  $\kappa_0$  for the entire range of  $\text{Re} = 5000 - 25,000$ , equal to 2. For simplicity,  $\kappa(x^0)$  as a function of  $\kappa_0$  to  $\kappa = 0$  was assumed to be linear, which virtually corresponds to the conditions of the experiment. The agreement between the theoretical curve calculated from (19) and the experimental curve should be regarded as satisfactory.

Our attention is drawn to the fact that with an increase in  $\kappa$  and  $\text{Re}$  the slope of the curve  $\lambda(\kappa, \text{Re})$  (Fig. 2) diminishes continually, which is particularly noticeable for the curve  $\kappa_0 = 2$ . A similar phenomenon was observed in the Koch experiment [10].

The resistance factor  $\lambda$  was measured in [6] for the range  $Re = (1-7) \cdot 10^5$  at various values of  $\alpha_0$ . The theoretical curves, calculated from (19), are in satisfactory agreement with the experimental data (Fig. 3).

#### NOTATION

$A = (\tau_{10}/\tau_{20})^2$ ; $B = \sqrt[4]{A/(1+A)}$ ; $C = \sqrt[4]{1/(1+A)}$	
$c_f$	is the frictional resistance factor;
$c_{f_0}$	is the value of $c_f$ when $x = 0$ ;
$D_0, E_0, k, L_0, M_1, M_2, M_3, M_4, n$	are constants;
$D = 1 + (2/z_1)R_X^{**}/(dR_X^{**}/dx)^{1/2}$ ; $E = 1 + H$ ; $L = k^2/z_2^2$ ; $H = \varphi_X^{**}/\varphi_X^{**}$	
$l$	is the mixing-path length;
$p$	is the pressure;
$P_1 = -U^{0'}/U^{02}Re$ ; $P_2 = -R^{0'}/R^0Re$ ; $Re = U_0R_0/\nu$ ; $Re_e = UR/\nu$	
$R$	is the radius of the channel wall;
$R_0$	is the value of $R$ when $x = 0$ ;
$R^0 = R/R_0$ ; $R^{0'} = dR^0/dx^0$ ; $r^0 = 1 - \delta/R$ ; $R_X^{**} = U\varphi_X^{**}/\nu R$ ; $R_{XY}^{**} = U\varphi_{XY}^{**}/\nu R$	
$u, w, \text{ and } v$	are the velocity components in the directions of the axes $x, \varphi, r$ ;
$u', w', \text{ and } v'$	are the turbulence pulsations of the velocity components;
$U$	is the value of the velocity $u$ outside of the boundary layer;
$U_0$	is the value of $U$ when $x = 0$ ;
$U^0 = U/U_0$ ; $U^{0'} = dU^0/dx^0$	
$w_0$	is the value of $w$ outside of the boundary layer;
$v_{1*} = \sqrt{\tau_{10}/\rho}$ ; $v_{2*} = \sqrt{\tau_{20}/\rho}$	
$x, \varphi, \text{ and } r$	are cylindrical coordinates;
$x^0 = x/R_0$ ; $y = R - r$ ; $y^0 = y/\delta$ ; $z_1 = kU/v_{1*}$ ; $z_2 = k\Gamma_1/\Gamma_*$	
$\delta$	is the thickness of the boundary layer;
$\Gamma = rw$ ; $\Gamma_1 = R w_0$ ; $\Gamma_* = R v_{2*}$	
$\theta$	is the half-angle of divergence for the diffuser;
$x = \Gamma_1/RU$	
$x_0$	is the value of $x$ when $x = 0$ ;
$\lambda$	is the channel resistance factor;
$\nu$	is the kinematic coefficient of viscosity;
$\rho$	is the density;
$\tau_1 \text{ and } \tau_2$	are the frictional stress components along the axis of rotation and in the circumferential direction, respectively;
$\tau_{10} \text{ and } \tau_{20}$	are the values of $\tau_1$ and $\tau_2$ at the channel wall;
$\chi = (z_1^2/k^2)R_X^{**}$	
$\chi_0$	is the value of $\chi$ when $x = 0$ ;
$\langle \rangle$	denotes averaging.

#### LITERATURE CITED

1. H. E. Weber, *J. Appl. Mech.*, **23**, No. 4 (1956).
2. M. A. Sinbel, *J. Appl. Mech.*, **26**, No. 4 (1959).
3. Yeh. Hsuan, *Trans. ASME*, **80**, No. 4 (1958).
4. N. E. Kochin, I. A. Kibel, and N. V. Roze, *Theoretical Hydromechanics, Part II* [in Russian], Fizmatgiz (1963).
5. A. H. Nissan and V. P. Breason, *A.I.Ch.E. Journal*, **7**, No. 4 (1961).
6. F. Liepe, *Maschinenbautechnik*, **12**, No. 3 (1963).
7. V. G. Shakhov, *Anniversary Science-Engineering Conference of the Kuibyshev Aviation Institute (Report Abstract)* (1967), pp. 61-62.
8. E. E. Solodkin and A. S. Ginevskii, *Trudy TsAGI*, No. 701 (1957).
9. Hoffman and Guber, in: *Mechanics* [Russian translation], No. 5, IL (1964).
10. R. Koch, *VDI, Forschungsheft* 469, Vol. 24 (1958).